Proceedings of the 6th JFPS International
Symposium on Fluid Power, TSUKUBA 2005
November 7-10, 2005

Dynamic Shear Flow of Electro-Rheological Fluids Between Two Rotating Parallel Disks

Masami Nakano*, Kiyotaka Yamashita*, Shinya Koizumi* and Ryosuke Keta*

* Department of Mechanical Systems Engineering, Faculty of Engineering
Yamagata University
4-3-16 Jonan, Yonezawa, Yamagata 992-8510, Japan
(E-mail: nakano@mnaka.yz.yamagata-u.ac.jp)

ABSTRACT

The transient response of induced shear stress and the related flow behavior of two types of the ER fluids containing particles have been investigated when they have been under the simultaneous stimulus of an constant DC or AC electric field and shear using a parallel rotary disk rheometer. For only one type of the ER fluid containing sulfonated polymer particles, as the electric field strength increases, the particles in the ER fluid form lamellar formations in the direction of shear, which may be responsible for the ER activity more than the strength of the chains. And, as the gap of parallel disks decreases down to about 0.1 mm, the particles gather around the outer edge of the disk to form a thick ring of the aggregation of the particles, which may be responsible for the increase of the shear stress. In this way, it would be expressed that the shear stress should change consistently with the morphology of the formations. In this work, the effects of shearing time, electric field strength, DC or AC, gap height between disk electrodes and types of ER fluid on the shear stress and the flow morphology are investigated.

KEY WORDS

Key words : Non-Newtonian Fluid, Electro-Rheological Fluid , Steady Shear Flow Mode, Dynamic Flow Behavior, Flow Morphology

NOMENCLATURE

E : Applied electric field strength of a parallel rotary disk rheometer ($=V/h$). In the case of AC electric field, E represents the amplitude of an applied AC electric field strength.
h : The gap height between two disk electrodes of the rotary rheometer.
$\dot{\gamma}$: The shear rate of the ER fluid flow defined at the outer edge of the disk.
τ : Induced shear stress
t : Shearing time

INTRODUCTION

Electrorheological (ER) fluids consisting of micron-sized polarizable particles dispersed in a dielectric liquid exhibit intriguing properties of yielding solids under the application of an electric field, which are associated with the alignment of the particles into a fibrous structure in the direction of the field due to electrostatic forces. The ER suspensions behave like a Bingham fluid having yield stress, which can be rapidly changed in reversible manner by applied electric fields [1]. So, ER fluids are known as a class of intelligent materials. These intelligent properties are anticipated

some applications of industrial devices such as dampers, valves, clutches, brakes, and so on. One of the problems presented by these fluids is hysteresis in flow-curves [2,3], which makes the precise control of the ER mechanical devices very difficult.

In this study, the transient response of induced shear stress and the related flow behavior of two types of the ER fluids containing particles have been investigated experimentally when they have been under the simultaneous stimulus of an constant DC or AC electric field and shear using a parallel rotary disk rheometer. The effects of shearing time, electric field strength, DC or AC, gap height between disk electrodes and types of ER fluid on the shear stress and the pattern formulation of the particles are investigated. This study is very important for the practical use of ER fluids in clutches and brakes.

EXPERIMENTAL APPARATUS AND MEASUREMENT SYSTEM

Two types of ER fluids were studied. One of them (TX-ER6 [4], 20 Vol%) is composed of numerously sulfonated polymer particles of average diameter of 5 μm suspended into silicone oil. Another one (FKER-V5, 35 Vol%) is composed of the composite type of organic and inorganic particles (average diameter 15 μm) dispersed into silicone oil.

As shown in Fig.1, the electrorheological properties of these fluids are evaluated by means of a rotary parallel disk rheometer (HAKKE, RheoStress RS150), in which an upper disk of 20 mm diameter rotates and a lower disk is fixed. A transparent glass disk electrode coated with ITO film of 38mm diameter replaces the lower disk, in order to enable to visualize the flow behavior from a bottom side. The gap between two parallel disks is set 0.1, 0.2, 0.3, 0.4, 0.5 and 0.7mm. An electric field is applied between two disk electrodes through a high voltage amplifier.

In the experiments, the shear rate $\dot{\gamma}$ defined at the outer edge of the disk is set a constant value of 100 s^{-1}, and the transient response of the induced shear stress and the pattern formulation of the particles are measured as a function of the gap height h and the DC and AC electric field strengths E.

TRANSIENT RESPONSE OF SHEAR STRESS AND FLOW PATTERNS

(a) TX-ER6 ER Fluid under DC Electric Field

Figure 2 shows the transient responses of the shear stress τ measured for the case of TX-ER6 ER fluid under the simultaneous stimulus of DC electric field and shear (h=0.2 mm, $\dot{\gamma}$=100 s^{-1}). The shear stress is

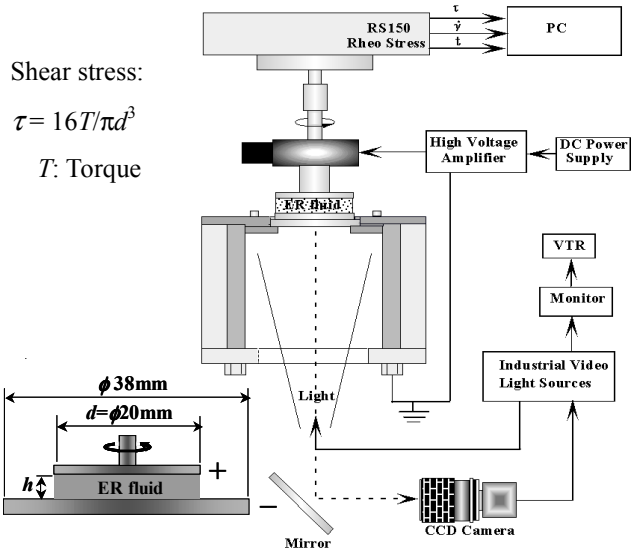

Fig.1 Experimental apparatus and measurement system using a rotary parallel disk rheometer

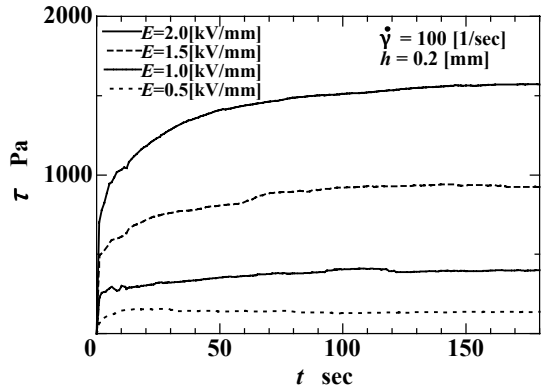

Fig.2 Time history of induced shear stress after simultaneous stimulus of constant shear and DC electric field (TX-ER6, h=0.2 mm, $\dot{\gamma}$=100 s^{-1})

suddenly increased just after the experiment is started and then is gradually increasing to approach a certain maximum value for every applied electric field strengths E. As the electric field strength is increased, this trend becomes remarkable and the maximum shear stress is increased due to the strengthened binding force acting between particles in the ER fluid. The maximum shear stress is increased in proportion to the square of the electric field strength.

As seen in Fig. 3 where the dark rings are composed of particles, the time variation of the shear stress can be explained by the evolution of the flow patterns with time. In the presence of an electric field, the particles align into a fibrous structure in the direction of the field due to electrostatic forces. When the ER fluid is sheared at a constant shear rate, at first the particles are uniformly dispersed between the disks, and then the

(a) t = 4 sec (b) t = 30 sec (c) t = 180 sec

Fig. 3 Structure evolution of ER fluid shear flow with time (E=2.0 kV/mm, h=0.2 mm, $\dot{\gamma}$ =100 s^{-1}, DC)

(a)E=0.5 kV/mm (b)E=1.0 kV/mm (c)E=2.0 kV/mm

Fig.4 Changes of ER fluid shear flow patterns with electric field strength (t=150 sec, h=0.2 mm, DC)

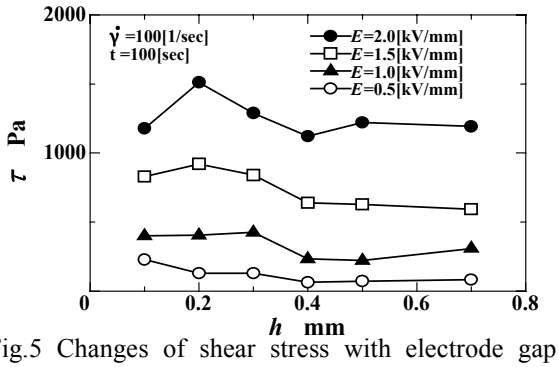

Fig.5 Changes of shear stress with electrode gap in terms of applied electric field strength (t=100 sec, DC)

(a)h=0.1 mm (b)h=0.2 mm (c)h=0.5 mm

Fig.6 Changes of ER fluid shear flow patterns with electrode gap (E=2.0 kV/mm, t=100 sec, DC)

particles are moved to the outer edge of the rotating disk, resulting in the lamellae formation having many thin rings inside the disk and a thick dark ring around the perimeter of the disk. The thickness of the dark ring is increased with time, indicating the particle gathering to the perimeter of the disk. As the results, the torque acting on the disk is increased and the induced shear stress is also increased. Thus, the morphology of the particle formations is closely related to the induced shear stress.

Figure 4 shows the effect of the electric field strength on the flow pattern of the ER fluid. As the electric field strength is increased, the thick dark ring around the perimeter of the disk becomes thicker.

Figure 5 shows the effects of gap of the electrodes on the shear stress (t=100sec). For the relatively narrow gap h of 0.3mm or less, the induced shear stress is a little larger than for the gap of 0.4 mm or more. In the case of the gap of 0.4 mm or more, the shear stress takes an almost constant value determined by the applied electric field strength E, independent of the gap. The effects of the gap h on the flow pattern are shown in Fig. 6. For the relatively large gap h of 0.5mm, the dark ring of the particles on the perimeter of the disk is not observed obviously and the lamellar rings of the particles are formed. The thick dark ring of the particles, which would cause the increase of the shear stress, is obviously observed in the case of relatively narrow gaps of 0.1 and 0.2 mm.

(b) TX-ER6 ER Fluid under AC Electric Field

Figure 7 shows the transient response of the induced shear stress τ measured for the case of TX-ER6 ER fluid in the presence of AC 10 Hz electric field (h=0.2 mm, $\dot{\gamma}$ =100 s^{-1}). The shear stress increases with increasing the electric field strength E due to the strengthened binding force acting between particles in the ER fluid, as well as the case of DC electric field. But the induced shear stress has an intense fluctuating

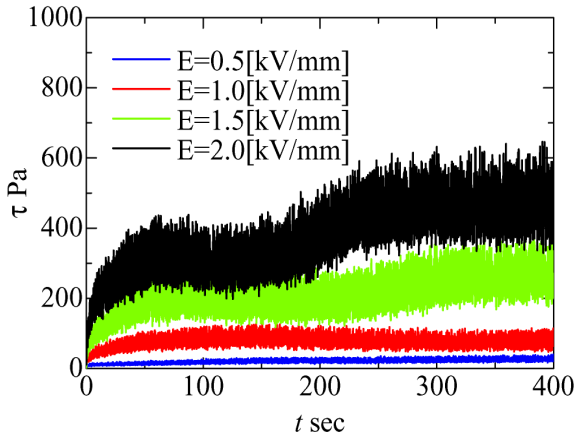

Fig.7 Time history of induced shear stress after simultaneous stimulus of constant shear and AC 10 Hz electric field (h=0.2 mm, $\dot{\gamma}$ =100 s^{-1})

(a) t = 3 sec (b) t = 25 sec (c) t = 200 sec

Fig. 8 Structure evolution of ER fluid shear flow with time (E=2.0 kV/mm, h=0.2 mm, $\dot{\gamma}$ =100 s^{-1}, AC10Hz)

component. The formation and destructions of fibrous structures of the particles might be caused alternately because of the applied AC electric field. The induced shear stress is smaller than that for the DC electric field case.

Figure 8 shows the transient response of the flow pattern of the ER fluid between the electrodes (AC 10Hz , E=2.0 kV/mm). As seen in Fig.8(a), (b), many thin rings inside the disk and a thick dark ring on the perimeter of the disk are observed at relatively early time, as well as the DC electric field case. The thick dark ring spreads inside with time, and finally a stable flow pattern is formed, consisting of one uniform circular structure of the particles inside the disk and a thin transparent ring of silicone oil on the perimeter of the disk, as observed in Fig.8(c).

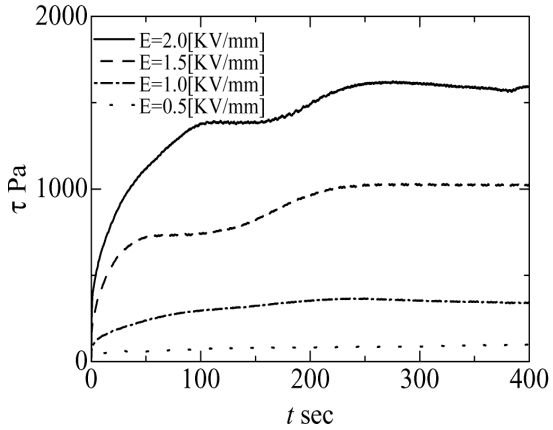

Fig.9 Time history of shear stress after simultaneous stimulus of constant shear and AC 50 Hz electric field (h=0.2 mm, $\dot{\gamma}$ =100 s^{-1})

(a) t = 3 sec (b) t = 25 sec (c) t = 200 sec

Fig. 10 Structure evolution of ER fluid shear flow with time (E=2.0 kV/mm, h=0.2 mm, $\dot{\gamma}$ =100 s^{-1}, AC50Hz)

(a)E=0.5 kV/mm (b)E=1.0 kV/mm (c)E=2.0 kV/mm

Fig. 11 Changes of ER fluid shear flow patterns with electric field strength (t=300 sec, h=0.2 mm, AC50Hz)

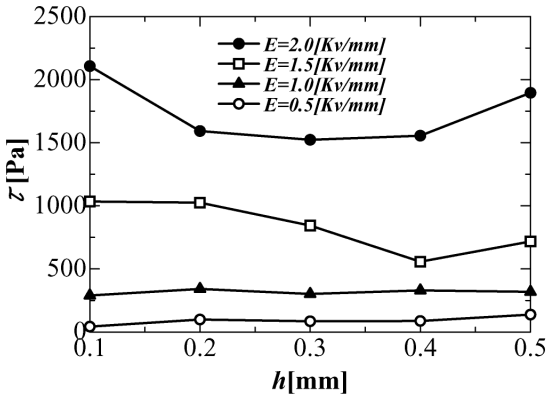

Fig.12 Changes of shear stress with electrode gap in terms of applied electric field strength (t=400 sec, AC 50Hz)

(a)h=0.1 mm (b)h=0.3 mm (c)h=0.5 mm

Fig.13 Changes of ER fluid shear flow patterns with electrode gap (E=2.0 kV/mm, t=400 sec, AC50Hz)

The transient responses of the induced shear stress τ measured in the presence of AC 50 Hz electric field (h=0.2 mm, $\dot{\gamma}$ =100 s^{-1}) are shown in Fig. 9. As the electric field strength increases, the shear stress increases in the same way as the DC electric field case. At relatively high electric field, the shear stress gradually increases with time and then settles at a constant value after a sufficiently long time. In this case, the intense fluctuations of the shear stress under AC 10Hz electric field are not observed because the formations and destructions of the fibrous structures of the particles might be caused alternately according to the AC frequency. The levels of the shear stress are greater than that for AC 10 Hz electric field case, and are almost the same levels as for the DC electric field case. The flow pattern evolution of ER fluid shear flow with time under AC 50Hz electric field strength is almost the same as the AC 10Hz electric field case, as seen in Fig.10. Figure 11 shows the effect of the electric field strength on the flow pattern of the ER fluid. The thick dark ring of the particles on the perimeter of the disk spreads inside to become thicker as the electric field strength increases, and at E=2.0 kV/mm the uniform circular structure of the particles is formed. So, it can be concluded that the dark ring on the perimeter of the disk spreads inside the disk to form the uniform circular structure in an earlier stage of shear as the electric field strength increases.

Figure 12 shows the effects of gap of the electrodes on the shear stress (t=400sec) for the case of AC 50 Hz electric field. It is obviously accepted that the induced shear stress do not significantly depend on the gap height, but for E=2.0 kV/mm the shear stress clearly increases at the relatively narrow gap of h=0.1 mm. It is found from Fig.13 that this increase of shear stress at h=0.1 mm might be due to the uniform circular structure of the particles spreading all over the disk, while at h=0.3mm and 0.5 mm the thin transparent ring of silicone oil appears on the perimeter of the disk as observed in Fig.13 (b), (c).

(c) FKER-V5 ER Fluid under DC Electric Field

Figure 14 shows the transient responses of the shear stress τ of the FKER-V5 ER fluid under DC electric field (h=0.2 mm, $\dot{\gamma}$=100 s^{-1}). The shear stress is suddenly increased just after the experiment is started and then maintains an almost constant value determined by the applied electric field strength, unlike the TX-ER6 ER fluid. That is, the shear stress of the FKER-V5 ER fluid under DC electric field does not exhibit any significant variation with time to keep a constant value. And unlike TX-ER6 ER fluid, the shear stress increases nearly in proportion to the electric field strengths ranging from 1.0 to 4.0 kV/mm, and is almost half as large as for TX-ER6 ER fluid.

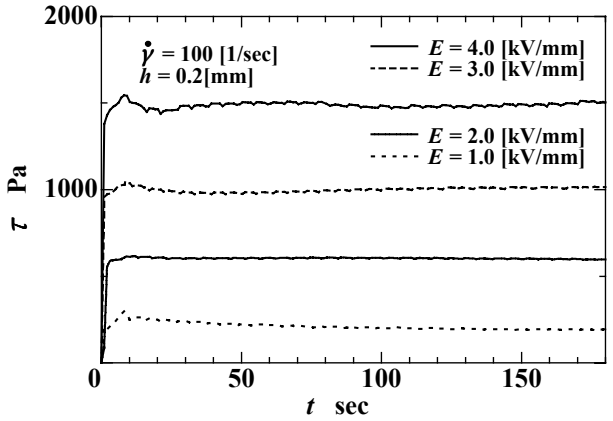

Fig.14 Time history of induced shear stress after simultaneous stimulus of constant shear and DC electric field (FKER-V5, h=0.2 mm, $\dot{\gamma}$=100 s^{-1})

(a) t= 4 sec (b) t= 30 sec (c) t= 180 sec

Fig.15 Structure evolution of ER fluid shear flow with time (E=4.0 kV/mm, h=0.2 mm, $\dot{\gamma}$=100 s^{-1},DC)

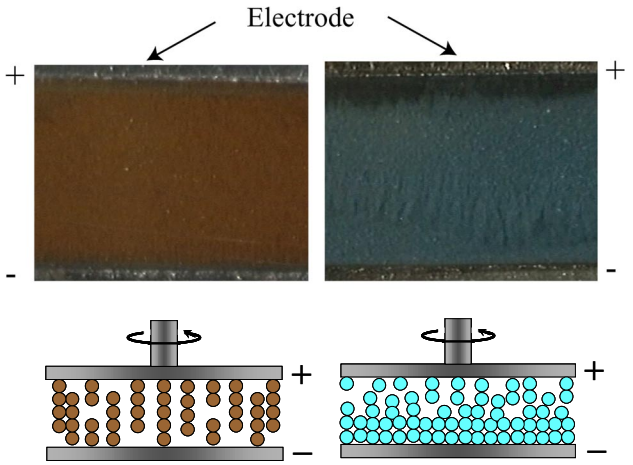

(a) TX-ER6 (b) FKER-V5

Fig. 16 Side-view of particles formation between two plane electrodes under electric field (h=2.0 mm, E=1.0 kV/mm), and schematic image of particles formation between two rotating disks

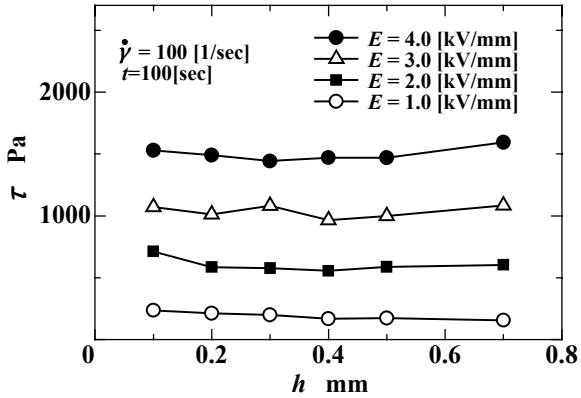

Fig.17 Changes of shear stress with electrode gap in terms of applied electric field strength (t=100 sec, DC)

As observed in Fig.15, the thick dark ring and the lamellar many rings of the particles, which appear in the case of TX-ER6 ER fluid, have never been observed. As shown in Fig. 16(b), in the case of FKER-V5, almost all particles could be observed to adhere to the GND electrode due to the electric charging of the particles under the DC electric field by the side-view visualization of particles behavior between two electrodes. Because of this, the particles are difficult to move easily to form the lamellar rings. While in the case of TX-ER6 ER fluid, because the chains of particles adhere to either of the electrodes as shown in Fig.16 (a), the particles might be easily moved to form the lamellar formations in the direction of shear.

The effects of the gap height h on the shear stress at t=100sec are shown in Figure 17. It can be concluded that the induced shear stress of the FKER-V5 ER fluid does not depend on the gap height h.

(d) FKER-V5 ER Fluid under AC Electric Field

Figure 18 shows the transient response of the shear stress τ measured for the case of FKER-V5 ER fluid under the simultaneous stimulus of AC 50 Hz electric field and shear (h=0.2 mm, E=1.0, 2.0, 3.0, 4.0 kV/mm, $\dot{\gamma}$=100 s^{-1}). The shear stress is suddenly increased just after the experiment is started and then is gradually increased to approach a certain maximum value, unlike the DC electric field. As the electric field strength increases, the shear stress also increases in the same manner as the DC electric field case. Figure 19 shows the flow pattern evolution of the ER fluid shear flow between the electrodes (E=4.0 kV/mm). Unlike the DC electric field case of Fig.15, very fine lamellar rings are formed all over the disk, but this flow pattern does not significantly change with time. When applied AC electric field, the polarity of the upper disk electrode changes alternately to be positive and negative as the lower electrode is grounded, so that the electric charged particles may easily move to upper or lower electrode according to the polarity of the upper electrode due to electrostatic forces, resulting in the formation of the very fine lamellar rings of the particles.

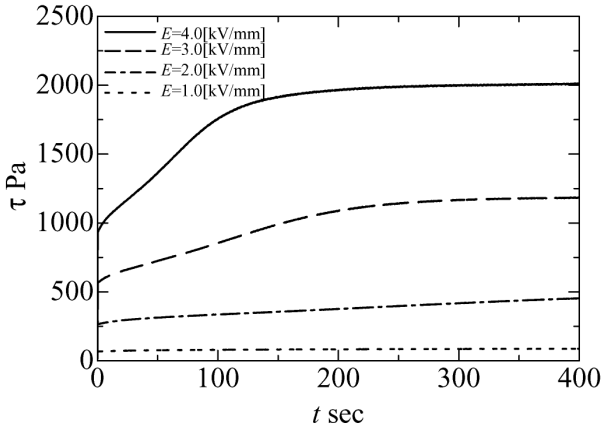

Fig.18 Time history of induced shear stress after simultaneous stimulus of constant shear and AC 50 Hz electric field (FKER-V5, h=0.2 mm, $\dot{\gamma}$=100 s^{-1})

(a) t = 3 sec (b) t = 25 sec (c) t = 200 sec

Fig. 19 Structure evolution of ER fluid shear flow with time (E=2.0 kV/mm, h=0.2 mm, $\dot{\gamma}$=100 s^{-1}, AC50Hz)

CONCLUDING REMERKS

We have experimentally studied the transient response of induced shear stress and the related dynamic flow behavior of two types of the ER fluids containing particles under the simultaneous stimulus of the constant DC or AC electric field and shear using a parallel rotary disk rheometer.

The ER fluid (TX-ER6) of numerously sulfonated polymer particles shows the remarkable time variations of the induced shear stress which increases gradually to saturate with time at relatively high electric field strength. It can be explained that the increase of the shear stress with time is due to the flow structure evolution to the lamellar formation of the particles in the direction of shear and the dense thick ring formation on the perimeter of the disk. Especially, as the electrode gap h decreases less than about 0.3 mm and the electric field strength E increases, the formation of the outer thick ring becomes remarkable and the thickness is increased with time, resulting in the increase of the shear stress. In the AC electric field of low frequency 10 Hz, the induced shear stress has an intense fluctuating component and shows a smaller value.

In the case of the ER fluid (FKER-V5) of organic and inorganic composite particles, we can not observed a big change in the flow structure because all of the dispersed particles adhere to one of the electrodes under DC electric field, so that the shear stress doesn't change with time and takes a stable value determined by the applied electric field strength. However, the induced shear stress is relatively low, about half of that for TX-ER6. While under AC electric field, the shear stress increases gradually with time in spite of almost no change of the flow structure.

ACKNOWLEDGEMENT

We would like to thank Mr. S. Yamamura for his assistance in the experiments.

REFERENCES

(1) M.Nakano, T.Yonekawa, Trans. of the Japan Society of Mechanical Engineers, **61**-581, (1995)B, 166-172, in Japanese.

(2) R. Aizawa, M. Nakano, et al., Int. J. of Modern Physics B, Vol. 15, Nos.6&7, (2001-3) 1070-1077.

(3) M. Nakano, K. Tsuge, T. Nagata, Proc. of 1st Int. Symp. on Advanced Fluid Information (AFI-2001), Sendai Japan, (2001-10) 498-501.

(4) Y. Asako, et al., Progress in Electrorheology, Havelka, K.O. and Filisko, F.E. eds., Plenum Press, (1995).